Phonon Localization and Dissipation in Polymer-like Disordered Systems

Louis Milhamont, Zhiting Tian, Samer Awale, Yann Chalopin

Phonon Localization and Dissipation in Polymer-like Disordered Systems

Louis Milhamont,[1] Zhiting Tian,[2] Samer Awale,[2] and Yann Chalopin[3,*]

[1] *Laboratory for Energetic, Macroscopic and Molecular, Combustion CentraleSupelec at University of Paris-Saclay Rue Joliot-Curie, Gif sur Yvettes*

[2] *Sibley School of Mechanical and Aerospace Engineering , Cornell University, Ithaca, New York 14853, United States*

[3] *Physics Department Laboratory for Structures, Properties and Modeling of Solids CentraleSupelec at University of Paris-Saclay Rue Joliot-Curie, Gif-sur-Yvettes*

(Dated: September 20, 2024)

The control of heat flow in disordered materials presents a significant challenge due to the limitations of conventional phonon transport models in systems lacking periodic long-range crystal order. This study investigates energy dissipation mechanisms induced by structural irregularities, utilizing folded polymers, particularly proteins, as model systems. Proteins, macromolecules characterized by coexisting periodic amino acid chains folded into irregular three-dimensional structures, serve as useful platforms for examining the impact of irregular topologies on vibrational properties. Our research reveals an important enhancement of the phonon density of states at mid-band frequencies, diverging from the Van Hove singularities typically expected at Brillouin zone edges in perfect crystals. This state redistribution exhibits similarities to observations in some disordered electronic and optical systems, generally known as Lifshitz tails. By interpreting this effect as a resonance between multiple degrees of freedom tuned by gradients of an effective phonon confinement potential, we provide a rational for interpreting the ubiquitous "Boson Peak" reported in disordered materials. Furthermore, this study elucidates how disorder allows heat to be channeled in narrow frequency bands. To this purposes, we present mathematical tools that enable rapid and sharp estimation of the phonon density of states and thermal currents, circumventing the need for solving expensive eigenvalue problems. Our methodology may facilitate the characterization and control of heat transport in specific amorphous and disordered solids, with implications for tailoring thermal materials through strategic manipulation of structural disorder.

I. INTRODUCTION

The study of energy transfers, particularly heat, has long been a focal point of scientific interest[1]. The thermal conduction properties of crystalline materials, characterized by their ordered structures, have been thoroughly investigated based on a comprehensive understanding of their phonon dispersion relations and scattering rates. These foundational insights have paved the way for accurate predictions of thermal properties[2,3]. However, in materials with structural disorder, long-range order vanishes, disrupting symmetries and invalidating the concept of a canonical Brillouin zone[4–9]. This structural disparity between crystals and 'glasses" consequently display stark contrast in thermal properties[4–8]. For instance, the vibrational energy landscape in amorphous silicon is complex, encompassing a range of modes like propagons, locons, and diffusons[4,10,11]. These modes defy simplistic classification, exhibiting characteristics that are neither entirely plane-wave-like nor localized[9,12]. Concurrently, investigations in various materials, such as higher manganese silicides, graphene, and superlattices, have revealed unexpected low-energy optical vibrational modes[9,13,14]. Central to these findings is the 'Boson Peak', a salient feature in the density of states of glasses and alloys, which has become a focal point of extensive research[15–26]. This phenomenon, characterized by an excess of vibrational modes at low frequencies, deviates from the Debye scaling and is observable even in supercooled liquids[27,28]. Despite these advancements, significant gaps remain in our understanding of the interplay between anomalous phonon density of states, localization phenomena, and the resulting diminution in thermal conductance in amorphous and disordered materials[29–31]. Fundamental questions arise regarding the principles governing energy dissipation in scenarios where structural disorder impedes phonon propagation and disrupts group velocities. Is there a unifying theory that can cohesively integrate the diverse observations and findings across various disordered materials? Recent advances in theoretical approaches are indeed moving towards a more unified understanding of disordered systems. Notably, the Wigner transport equation approach[32] and quasi-harmonic Green-Kubo methods[33,34] have shown promise in bridging the gap between ordered and disordered materials. The Wigner formalism, by treating phonons as partially coherent waves, provides insights into the transition between ballistic and diffusive transport regimes. Similarly, the quasi-harmonic Green-Kubo approach offers a framework to calculate thermal conductivity in both crystalline and amorphous materials within a single formalism. While these methods represent significant progress, our work complements these approaches by focusing on the spatial aspects of energy localization and

transport, particularly in systems with complex topologies like folded proteins.

By employing the mathematical framework of the localization landscape[35] extended to phonon systems[36,37], we conduct a systematic examination of energy dissipation in disordered phonon systems[38]. Our focus is on folded proteins, which, with their intrinsic mix of periodicity modulated by topological irregularities, provide an ideal model for our investigation[18]. Our findings, based on dimensionality-reduced model reveal features that may be applicable to a range of disordered solids under specific conditions, particularly those ensuring coherence in phonon transport.

II. METHODS

In this Methods section, we present a comprehensive framework for analyzing thermal phonons in disordered systems, with a particular focus on folded proteins as model structures. Our approach combines several key elements: (1) a generalized equation of motion for vibrational dynamics in random media, (2) the innovative application of the localization landscape concept to phonon systems, (3) a novel method for estimating the density of states based on the effective confinement potential, and (4) calculations of heat flux between degrees of freedom. We begin by introducing the fundamental equations governing the system's dynamics, then explain how we adapt the localization landscape to phonon systems. Subsequently, we detail our approach to spectral decomposition and heat flux calculations. Finally, we describe our method for estimating the density of states and heat capacity. Throughout, we emphasize how these tools allow us to predict and understand energy localization and transport in disordered structures without resorting to computationally expensive eigenvalue calculations.

Our description of thermal phonons in disordered systems is primarily guided by a mathematical framework within the harmonic approximation. We consider the vibrational dynamics of discrete systems within a random medium, accounting for inhomogeneous linear coupling between degrees of freedom.

Equation of Motion

We begin with the fundamental equation of motion of coupled harmonic oscillators:

$$\omega^2 \tilde{X}_i = \left(\sum_{j\sim i} \frac{k_{ij}}{m_i} \right) \tilde{X}_i - \sum_{j\sim i} \frac{k_{ij}}{\sqrt{m_i m_j}} \tilde{X}_j \qquad (1)$$

This equation can be interpreted as follows:

- $\omega^2 \tilde{X}_i$: Represents the acceleration of the i-th degree of freedom.
- $\left(\sum_{j\sim i} \frac{k_{ij}}{m_i} \right) \tilde{X}_i$: Describes the restoring force on the i-th degree of freedom due to its own displacement.
- $-\sum_{j\sim i} \frac{k_{ij}}{\sqrt{m_i m_j}} \tilde{X}_j$: Represents the influence of neighboring degrees of freedom.

Here, k_{ij} is the coupling constant between the i-th and j-th degrees of freedom, m_i denotes the mass associated with the i-th degree of freedom, and ω represents the vibrational frequency corresponding to the displacement $\tilde{X}_i$. This formulation generalizes the standard equation of motion for a simple harmonic oscillator by integrating terms that encapsulate the influence of neighboring entities in random environments.

Localization Landscape Approach

The force constants are determined with a parameter-free elastic network model[39]. We can cast this in the form of an eigenvalue problem:

$$L_h \tilde{X} = (C - \omega^2)\tilde{X} \qquad (2)$$

where $L_h = -[\mathrm{div}(A\nabla) - V]$.

Using a mathematical tool termed the localization landscape (LL) u[35], we can access the localized distributions of normal modes by solving:

$$-[\nabla \cdot (A\nabla) - V]u = (1) \qquad (3)$$

where (1) is a column vector, $A : (\alpha_{ij}) = (-1)^{i-j} k_{ij}$, since $e^{\boldsymbol{i}\pi(i\cdot a - j\cdot a)/a} = (-1)^{i-j}$ for a modulated structure of period a and V is the difference between the diagonal and off-diagonal elements (See SI[40] for details).

Generalized Wave Equation

Introducing $\tilde{X} = u\phi$ to account for the modulation of the mode with an envelope defined by u, and using $W = \frac{1}{u}$ and $\Omega^2 = C - \omega^2$, we eventually arrive at:

$$\left[-\nabla \cdot (A\nabla) + 2A\frac{\nabla W}{W} \cdot \nabla + (W - \Omega^2) \right] \phi = 0 \qquad (4)$$

This equation contains three key terms:

- $-\nabla \cdot (A\nabla)$: It represents the propagation of waves through the medium. It's analogous to the diffusion term in other physical systems
- $2A\frac{\nabla W}{W} \cdot \nabla$: A convecto-diffusive term describing energy transport influenced by the landscape's structure. It represents how the wave is influenced by spatial variations in the effective potential W. This term is responsible for directing the energy flow in the system.

- $(W - \Omega^2)$: A confinement potential term that localizes waves. This term acts as an effective potential that confines the waves. W is the inverse of the localization landscape, and Ω^2 is related to the frequency. The interplay between these two determines, as for an effective barrier, where modes are likely to be localized.

Equation 4 captures the competition between wave propagation, energy transport influenced by the landscape's structure, and localization effects in disordered systems. It's a powerful formulation that combines aspects of wave physics, transport phenomena, and quantum mechanics to describe phonon behavior in complex, disordered materials.

Visualization of Key Quantities in 3D Protein Structures

Figure 1 illustrates how the various quantities encountered in our equations project onto a 3D color-coded structure, using a folded hydrogenase protein as an example (Figure 1a). The confinement potential, shown in Figure 1b, indicates regions where energy is likely to be confined or trapped along the protein chain at the extrema of the potential W. This potential plays a crucial role in determining the localization of vibrational modes.

An alternative visualization of this potential's effect is presented in Figure 1e. Here, we plot the eigenvectors of the system, ranked as a function of their corresponding eigenvalues. This representation reveals that the amplitudes of the eigenvectors are fully modulated by the confinement potential, analogous to wave functions in a quantum well. Figure 1c visualizes the gradient of the confinement potential. This quantity is intrinsically linked to energy transport within the system. As we will demonstrate later, it corresponds to the resistance to heat flow, providing insight into the thermal conductivity of the protein structure. The inverse of the confinement potential, depicted in Figure 1d, serves as an estimate of the phonon density of states (see[40] for a complete demonstration). This relationship, which we will address in subsequent sections, offers a computationally efficient method to approximate the vibrational spectrum of the protein.

Heat Flux Calculation

We begin by discriminating domains defined by the maxima of W and comparing the behavior in regions where ∇W is most significant. To benchmark our approach, we first calculate the heat flux between two degrees of freedom (DoF) across the entire frequency spectrum using the established method of Matsuda et al.[41]:

$$q_h^{ij} = k_{\mathrm{B}}(\mathrm{T}_j - \mathrm{T}_i) \sum_n \frac{|Y_i|^2 |Y_j|^2}{|Y_i|^2 + |Y_j|^2} = k_{\mathrm{B}}(\mathrm{T}_j - \mathrm{T}_i)\mathbb{T}_{ij} \quad (5)$$

where k_{B} is the Boltzmann constant, T_i and T_j are temperatures of the i-th and j-th DoF, Y_i and Y_j are their respective eigenvector components, and $\mathbb{T}_{ij}$ represents the transmission coefficient.

Novel Approach: Heat Flux from Confinement Potential

We demonstrate that the gradient of the confinement potential W corresponds to the resistance to heat flow. This allows us to compute the inverse quantity of what is obtained from Eq. 5, without solving the complete eigenproblem. Our method relies solely on the knowledge of ∇W, offering significant computational advantages.

Density of States Estimation

To elucidate the vibrational properties of the system, we employ three distinct methods to calculate the density of states (DoS). Specifically, these methods entail: (1) the eigenvalue spectrum of L_h, (2) Weyl's law for the counting function, as elucidated by Arnold[42], and (3) a novel approach predicated on the curvature of W. Notably, our method for estimating the DoS exhibits enhanced speed compared to directly solving the eigenproblem. The analytical expression derived from this approach is detailed in the Supplementary Information[40] :

$$g_\nabla(\omega^2) = \sum_{(x_1,x_2)\in S_{\omega^2}} \frac{1}{\nabla W(x_2)} + \frac{1}{\nabla W(x_1)} \quad (6)$$

where S_{ω^2} is defined as:

$$S_{\omega^2} = \left\{(x_1, x_2) \in \Omega \times \Omega \quad \middle| \quad x_1 < x_2, W(x_1) = W(x_2) = \omega^2, \forall x \in (x_1, x_2),\, W(x) < \omega^2\right\} \quad (7)$$

This DoS estimation method is computationally efficient, particularly valuable for large, complex systems.

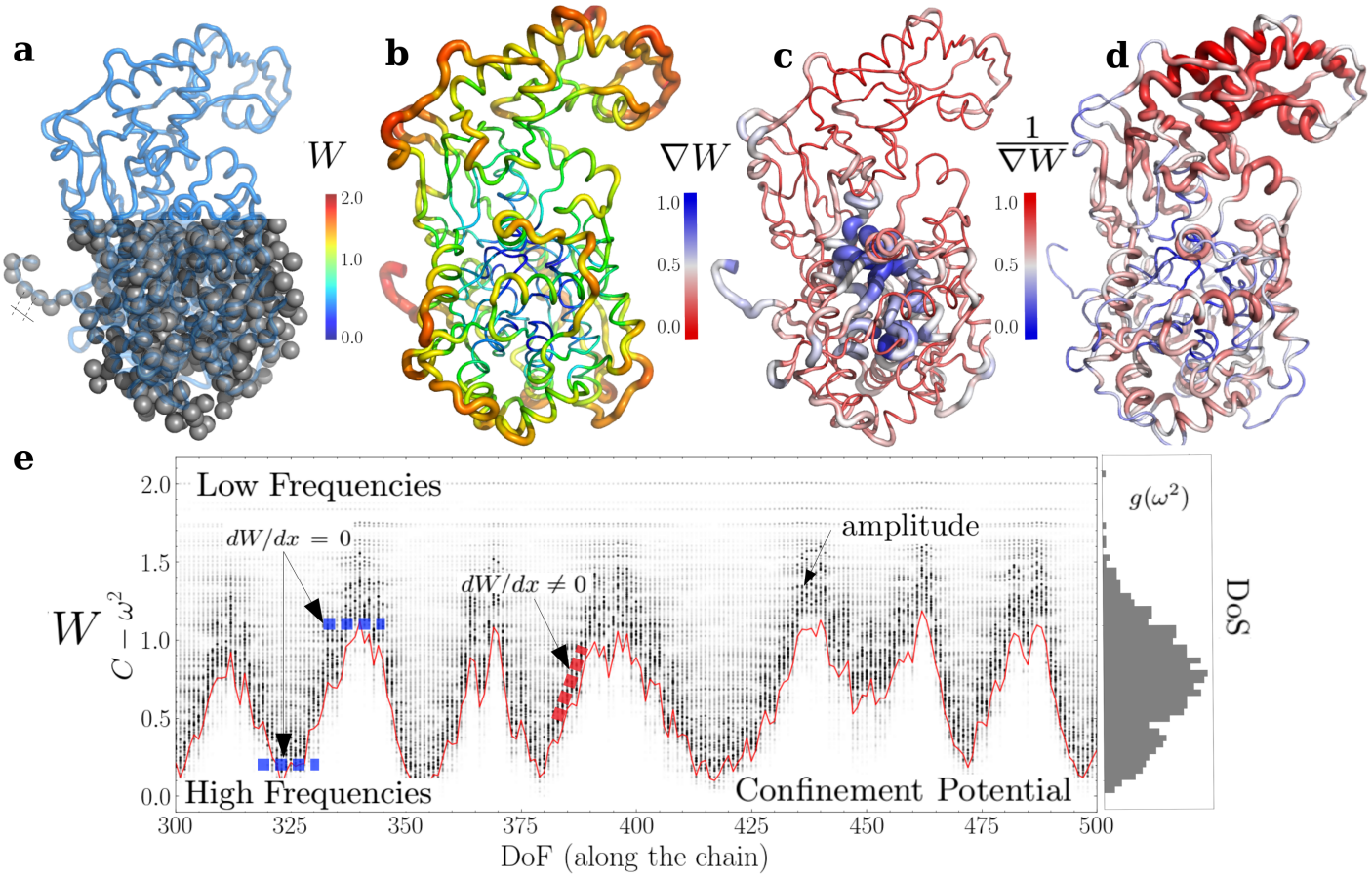

FIG. (1) **Localization Phenomena in a Model of Disordered Structure: A Folded Protein.** a) A three-dimensional depiction of the hydrogenase protein chain with PDB ID 4xdc, showcasing the cohexistence of periodicity and disorder. b) The effective confining potential W with highlighted high-frequency localized modes (in red) and low-frequency localized modes (in blue). c) A color-coded three-dimensional visualization based on the gradient of the effective potential. This highlights the core region dominated by high-frequency vibrations and the external regions characterized by low-frequency vibrations. e) A 3D representation of the inverse gradient of the effective potential ($1/\nabla W$). This visualizes the primary thermally conductive degrees of freedom, emphasizing the local density of states derived from the gradient operator. e) The effective heat confinement potential W (in red) computed for the chain's 581 Degrees of Freedom (DoF). This is juxtaposed with the corresponding normal modes (in grey) and the eigenmodes spectrum (DoS) to highlight confinment effects.

Heat Capacity and the Boson Peak in Disordered Systems

The heat capacity is a crucial experimental quantity often investigated to capture the essence of disorder in materials. Its deviation from the Debye law, particularly the excess of low-frequency modes known as the Boson peak, provides evidence that disorder has compromised phonon dispersion. We now extend our analysis to include this important thermodynamic property. Once the eigenvalue problem is solved, we can compute the heat capacity of the protein in the harmonic approximation:

$$c_V = \frac{\partial U}{\partial T} = \sum_n \frac{\hbar^2 \omega_n^2}{k_B T^2} \frac{e^{\frac{\hbar\omega_n}{k_B T}}}{(e^{\frac{\hbar\omega_n}{k_B T}} - 1)^2} \tag{8}$$

where U is the internal energy, T is the temperature, ω_n are the eigenfrequencies, and k_B is the Boltzmann constant.

Einstein-like Model for Discrete Systems

Introducing $\theta_n = \frac{\hbar\omega_n}{k_B}$ as the characteristic temperatures of the modes, we obtain a heat capacity expression similar to Einstein's model, reflecting the discrete nature of the protein system:

$$c_V = k_B \sum_n \left(\frac{\theta_n}{T}\right)^2 \frac{e^{\frac{\theta_n}{T}}}{\left(e^{\frac{\theta_n}{T}} - 1\right)^2} \tag{9}$$

Low and High Temperature Limits

In the low temperature limit, where $T \ll \theta_m = \min_n \theta_n$, the behavior resembles Einstein's model:

$$c_V \underset{T \ll \theta_m}{\sim} k_B \frac{\theta_m^2}{T^2} e^{-\frac{\theta_m}{T}} \tag{10}$$

In the high temperature limit, where $T \gg \theta_M = \max_n \theta_n$, we recover the Dulong-Petit law:

$$c_V \underset{T \gg \theta_M}{\sim} N k_B \tag{11}$$

where N is the number of degrees of freedom.

Application to Proteins and Disordered Structures

Our focus on disordered structures like proteins and enzymes is particularly relevant for several reasons:

- Proteins, despite their irregular 3D topology, possess an intrinsic periodicity of $3.8\mathring{A}$ along the polypeptide chain, making them ideal models for studying phononic properties in disordered materials. While the elastic model accounted in this study and similar elastic network models are based on 3D protein structures, they often employ simplifications that result in effectively 1D representations of protein dynamics. This includes treating residue fluctuations as scalar quantities and focusing on nearest-neighbor interactions along the protein chain. However, it's crucial to note that these models still capture essential 3D structural information through their initial construction from the protein's spatial configuration. Importantly, treating the system with a full 3D elastic tensor does not fundamentally alter the underlying physics or the shape of the confinement potential[36]. The use of a simplified 1D-like model grants mathematical simplicity in our demonstrations without sacrificing the essential physical insights. This simplification allows us to elucidate key principles of protein dynamics while maintaining analytical tractability. The core behaviors observed in our model, such as the relationships between the potential gradient, density of states, and heat flux, remain valid when considering the full 3D elastic properties of the protein structure.

- Their naturally occurring structures are well-documented in databases like CSA (Catalytic Site Atlas), providing a rich source of data for analysis.

- Simplified elastic interaction models[43] have proven effective in describing normal modes of proteins[44], and we leverage these models in our study. It's important to note that our model employs a coarse-grained representation, with each amino acid treated as a single degree of freedom. While this approach reduces the total number of degrees of freedom compared to an all-atom model, it captures the essential dynamics relevant to energy storage and transport. The periodicity of the protein backbone chain defines the Brillouin zone in our model, while the influence of side chain atoms is indirectly accounted for through scaled force constants. This approach has been validated against molecular dynamics simulations, with Debye-Waller factors showing over 80% correlation between our model and full atomistic simulations[45]. This high correlation suggests that our coarse-grained model effectively captures the key physical behaviors of protein dynamics while allowing for the study of larger systems and longer time scales.

Significance and Future Directions

The analysis of protein heat capacity offers several significant implications. By examining the heat capacity of proteins, we can identify deviations from the Debye law, particularly the Boson peak, which is indicative of an excess of low-frequency modes characteristic of disordered systems. This analysis also provides valuable insights into how structural disorder affects vibrational properties and energy transport in complex biomolecules. Furthermore, it may potentially establish connections between localization phenomena, as described by our confinement potential approach, and macroscopic thermodynamic properties.

In this context, we define "low temperature" as any temperature below the Debye temperature (Θ_D). The Debye temperature represents the highest normal mode of vibration in a crystal, and in the harmonic approximation, it is given by $\Theta_D = \hbar\omega_D/k_B$, where ω_D is the Debye frequency. Given that our vibrational density of states extends up to 4 THz, we can estimate the Debye temperature as $\Theta_D \approx \hbar(2\pi \times 4 \times 10^{12})/k_B \approx 192$ K. Therefore, in our analysis, temperatures significantly below 192 K are considered "low temperatures," where quantum effects become increasingly important and the system's behavior deviates from classical predictions.

III. RESULTS

In the intricate realm of molecular structures, proteins epitomize a fascinating interplay between order and disorder. When folded, they adopt an irregular 3D conformation, akin to polymers, as illustrated in Figure 1a. Such spatial complexities, far from being mere anomalies, often underpin protein functions[39]. Concurrently, the protein maintains a periodicity in its amino acid arrange-

ment, marked by a consistent $a = 3.8\mathring{A}$ period defining the wave-vector $k = 2\pi/a$.

A. Model

To delve deeper into this balance, we examine a specific protein (PDB id 4xdc) composed of 581 amino acids, treating each amino acid as a degree of freedom. Later discussions will underscore that size or the number of DoF does not influence our final conclusion. This protein serves as our model for studying disordered phonon systems. For disordered phonon systems meeting the criteria of harmonicity and coherence, our approach conceptualizes the dynamics as a coexistence between wave propagation or diffusion and wave localization, with modal amplitudes decreasing exponentially due to structural disorder (as described in eq.4). Central to our investigation are the positions of the carbon C_α atoms, pinpointed with a $1.6\mathring{A}$ resolution via X-ray diffraction[46], as showcased in Figure 1a.

B. Localization Landscape Analysis

We compute the localization landscape (eq. 3) and focus on its inverse ($W = 1/u$) which acts as an effective confinement potential for eigenmodes[37,42]. This allow us to

- partition the vibrations into distinct subdomains
- Observe eigemodes modulation by the potential's boundaries(Figures 1b and 1c).

As key observation, we found that high frequencies predominantly localize within the protein's core, indicative of stiffer regions. In contrast, external, soft degrees of freedom (DoF) exhibit diminished cohesive energy[37] and display lower frequency motions. This underscore the pivotal role of topology in the spatial localization of energy.

C. Heat Flux Analysis

Our investigation computes the heat exchanges occurring between all degrees of freedom, as visualized in Figure 2. Unlike conventional crystals, the heat flux in our structure is not uniformly distributed. Instead, we observe:

- A pronounced inhomogeneity in heat flux coupling between different domains, with a variance of half an order of magnitude (Figure 2a).
- A distinct dissipation network emerges (Figure 2b).
- The underlying influence of topology on this network is evident (Figure 2e).
- Heightened heat flux in regions where the potential increases rapidly.

D. Energy Equipartition

The observed variations in heat flux along the chain are consistent with energy equipartition, reflecting the dynamic nature of energy exchange between degrees of freedom. While instantaneous local fluxes may vary, each degree of freedom maintains the same average energy over time. This can be verified by examining the normal modes across the entire frequency spectrum, ensuring that each degree of freedom carries, on average, the same amount of vibrational energy $< E_i >$(with $< E_i >= 1/2 \sum_n m_i \omega_n^2 X_{i,n}^2$, for each eigenstate n).

This analysis examines how protein structure may affect phonon localization and heat dissipation. The coexistence of order and disorder in proteins could potentially create distinct patterns of energy distribution and transport, offering insights into the intricate dynamics of certain disordered systems.

E. Efficient Conductors and Energy Transfer

By progressively setting a specific heat flux threshold, we identify the emergence of most efficient conductors and their positions within the confinement potential. As shown in Figure 2d, these efficient conductors primarily occupy the mid-range of the confinement potential, corresponding to the mid-frequency range of the phonon spectrum.

To understand the underlying mechanisms, we examine the vibrational energy mismatches between each degree of freedom (DoF) using the operator $|\nabla W|$. We quantify this by computing $\|\nabla W_i\|_2$, applying the L2 norm to $|\nabla W|$ to assess the local energy gap (Figure 1c).

To elucidate the underlying mechanisms, we investigate the vibrational energy mismatches between each degree of freedom (DoF) by employing the operator $|\nabla W|$. This is quantified by computing $\|\nabla W_i\|_2$, which involves applying the L2 norm to $|\nabla W|$ to assess the local energy gap (Figure 1c). The gradient operator, defined for a graph (see SI[40]), balances vibrational frequency mismatch and topological proximity between DoF. Our key observations include the following: high and low frequency regions exhibit sparse energy states that localize on specific DoF, resulting in elevated ∇W values; the mid-localization band is characterized by ∇W peaks where $W \approx 0.5$; and sequence coordinates, due to inhomogeneous coupling, display rapid oscillations, which intensify localized vibrational states around the mid-localization band. High values in this metric indicate inefficient heat transfer, while low values suggest efficient heat exchange (Figure 2c). This phenomenon, where increased disorder along sequence coordinates enhances localized states' resonance to form a thermal channel, is

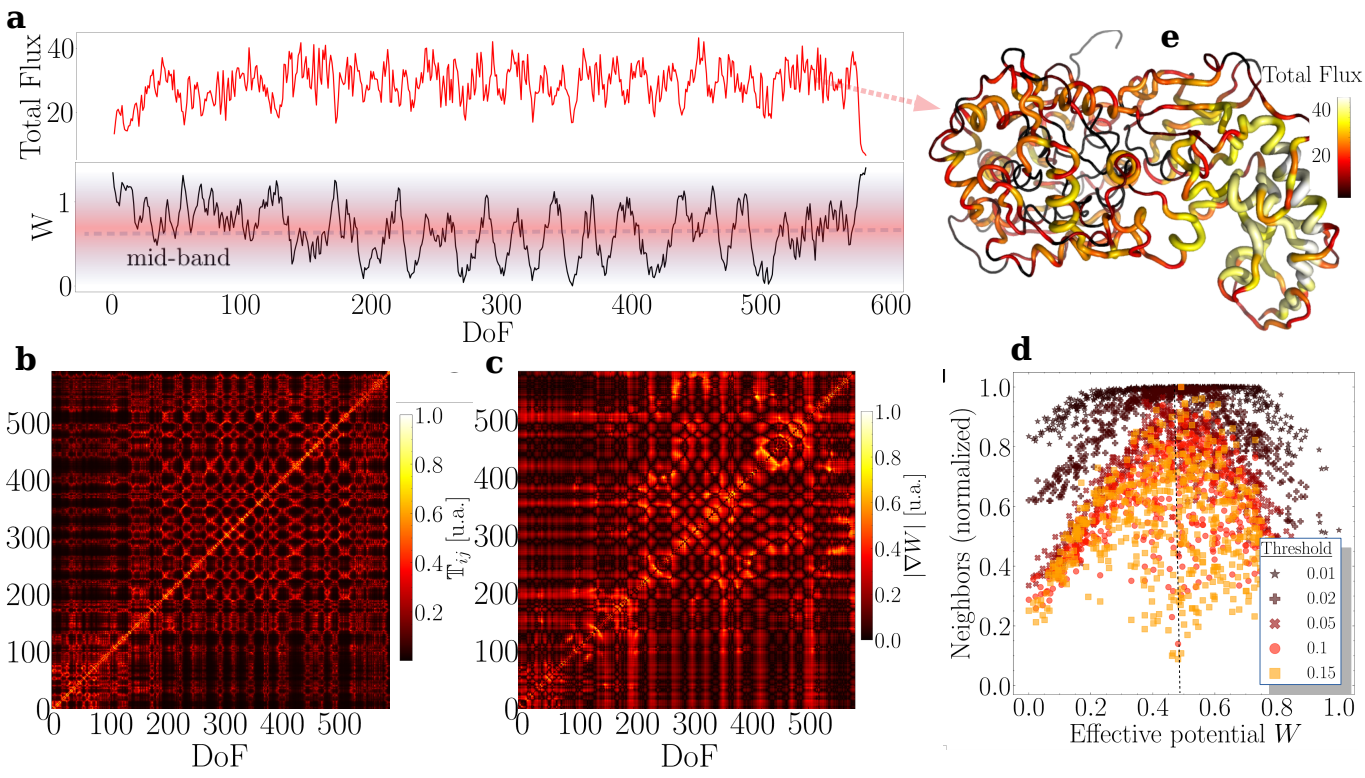

FIG. (2) **Energy Transfers in a Disordered Folded Protein.** a) Bottom: Depicts the effective heat confinement potential (in red). Top: Represents the total flux per degree of freedom (DoF), highlighting a partial correlation with the confinement potential. b) Visualizes the heat conductance between each DoF, emphasizing the diverse thermal channels within the structure. c) Estimates the system's thermal resistance, which inversely correlates with the heat conductance shown in (b). d) Demonstrates the count of thermally coupled DoFs against an energy threshold (ω^2), indicating that optimal conductors emerge around the confinement potential's midpoint (approximately ~ 0.5). e) 3D representation of the total flux per DoF.

termed the 'thermal lens'.

F. Density of States and Anisotropic Conduction

We introduce a novel method for estimating the density of states (DoS) based on the effective confinement potential. The DoS, denoted by $g_\nabla(\omega^2)$, correlates with the local gradient of the confining potential at a specific energy state, as detailed in SI. Our method is validated by comparing it with benchmark calculations, including the dynamical matrix's spectra and Weyl's law counting function, as shown in Figure 3b. The key findings from this analysis are as follows: the DoS features pronounced peaks around a normalized vibrational energy value of ~ 0.7, which locate around the mid-band of the phonon spectra; the density deviates from systems with an acoustic mode dispersion relation, lacking the expected Van Hove singularity at the zone edge; protein chain folding introduces additional vibrational frequencies due to lateral interactions, leading to flat branches akin to Einstein oscillators; and these branches contribute to a broadened density of states, appearing as a variant of the Van Hove singularity at lower frequencies. Notably, our findings align with the notion that the Boson Peak can be viewed as a modified form of the Van Hove singularity in certain disordered systems, as discussed by Chumakov[47]. Furthermore, the system's frequency-dependent thermal conductance aligns with the DoS results, demonstrating that degrees of freedom at the smoothest potential gradients have the highest heat dissipation capacity, as illustrated in Figure 3a. This investigation elucidates remarkable analogies between the vibrational characteristics of protein structures and well-established paradigms in discrete electronic transport systems. We observe the manifestation of Lifshitz tails, characterized by a diminished density of states (DoS) at both the Brillouin zone center and periphery, closely mirroring phenomena documented in electronic systems[48–51]. Of particular significance is the discovery of a pronounced DoS concentration toward the mid-band region, which facilitates the propagation of conductive coherent states. This distribution pattern emerges in the absence of spectral gaps, a distinctive feature that, while differentiating our findings, maintains conceptual concordance with electronic transport models. The observed mid-band shift of DoS

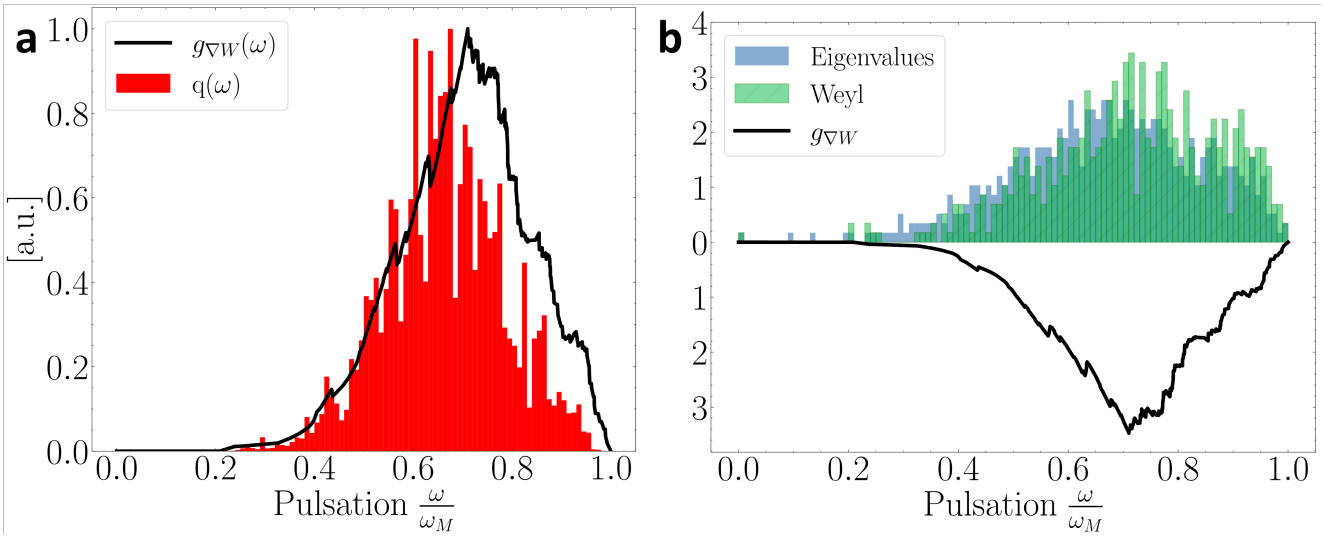

FIG. (3) **Phonon Density of States in a Disordered Protein Structure.** a) A comparison of the density of states based on the system's eigenfrequencies with the frequency-dependent heat flux. Pulsations are normalized by the maximum value, ω_M. b) Benchmark methods for determining the Density of States (DoS) are evaluated: Eigenfrequencies without approximation (blue); the Weyl law derived from a counting function[42] (black); and our proposed estimation using the operator ∇W (black). The correlation coefficients between the eigenvalues method and the Weyl law, and the ∇W method are 0.85 and 0.92, respectively, highlighting the effectiveness of our operator.

and its role in enabling coherent transport resonates with analogous phenomena in electronic systems, suggesting a fundamental commonality in the influence of structural disorder on energy transport across diverse physical domains.

G. Heat Capacity and Boson Peak

We examine the heat capacity behavior ($C_v(T)$) in comparison to the Einstein and Debye models. Figure 4a displays the temperature-dependent C_v trends obtained from eq.9 compared to both models. For the Einstein model, we consider the frequency corresponding to the density of state's maximum ($W \sim 0.7$) whereas for the Debye model we employ the parameters θ_D and the number of degree of freedom N. What comes out is that in a folded periodic structure C_v deviates from the Debye scaling law and aligns closely with the Einstein model.

Disorder tends to spatially decouple domains while consolidating these decoupled harmonic domains into quasi-single frequency resonators. The DoS structure comprises a compact ensemble of Dirac deltas, forming an asymmetric Gaussian distribution peaking at $\omega \sim 0.7$.

Figure 4c visualizes deviations from the Debye law by renormalizing C_v with T^d. Here, $d = 1$. A distinct peak, known as the Boson Peak, spans a temperature range aligning with the equivalent temperature defining the density of states' spectral support. This peak represents the excess in the density of states resulting from crystal symmetry disruption.

To ensure robustness, we analyzed 10 distinct proteins with high spatial resolution, finding minimal statistical dispersion (Figure 4d).

IV. DISCUSSION

A. Distinctive Density of States and Its Implications

Our study reveals a unusual characteristic in the density of states (DoS) of polymer-like disordered phonon systems: resonant peaks shifted to lower frequencies than predicted by the Van Hove singularity. This observation serves as a predictive tool for the structure factor in such systems. It's important to note that any experiments involving the measurement of these protein properties would typically involve either crystallized proteins, as in Cryo-EM or X-ray diffraction studies, or proteins in solution at concentrations close to saturation. These conditions are necessary for the structure factor to be meaningful and measurable. In this context, we anticipate that localized and coherent resonnant vibrational modes will predominantly exhibit two type of structures:

- Flat, high and low-frequency branches indicative of localized state at the extrema of the phonon spectra[18], that is a pronounced $\Delta k >> 2\pi/L$ due to localization ($\Delta x << 1$)
- A bright point close to the mid-band corresponding the resonant modes driving coherent energy trans-

port. One can possibly predict that this mid-band frequencies might also coincide with $\nu \sim V_g/L$, where L is the protein length and V_g is the bulk group velocity derived from amino acids interaction energy in the case where it is unfolded.

These predictions may prove to be possibly relevant for predicting and interpreting experimental data obtained from highly concentrated or crystallized protein samples.

B. Analytical Tools and Heat Transfer Mechanisms

To probe these phenomena, we introduced the operator $|\nabla W|$, specifically designed for graph systems. This operator measures a structure's resistance to heat flow, eliminating the need for resolving the eigenvalue problem or accessing the Green's function. It identifies inefficient heat transfer pathways, characterized by high $|\nabla W|_{i,j}$ values, and correlates inversely with the local density of states, which is crucial for heat transfer orchestration. This approach offers enhanced efficiency and predictive power compared to traditional methods, as demonstrated in Figure 1d.

C. The Role of Confinement Potential

A key finding is the significance of the confinement potential's gradient (Figures 2a and 3a) to understand thermal properties of our system.

The potential gradient (∇W) reaches its maximum for low and high-frequency modes, as the degrees of freedom associated with these extreme energies are surrounded by neighbors with significantly different energies. Moreover, the inverse of ∇W is proportional to the density of states (DOS), since a low ∇W indicates that the DoF is surrounded by neighbors with similar energies, corresponding to a high DOS. Given that the DOS is directly related to heat flux, we can establish that ∇W is inversely proportional to the local thermal conductivity. The intermediate region of the energy band, corresponding to amino acids located between the core and the surface of proteins, exhibits a relatively low ∇W (see Figure 1c). Consequently, this region facilitates efficient coherent heat transport through quasi resonant degrees promoting a sharp density of state and corresponding to domains located distally.

Hence, The confinement potential acts as a spectral lens, concentrating numerous degrees of freedom to spectrally synchronize, particularly in the middle frequency domain when structural disorder is introduced.

D. Thermal Behavior and the Einstein Model

Proteins exhibit a unique coherent effect in their disordered phonon systems, deviating significantly from the conventional Debye model in heat capacity analysis. This phenomenon arises from the protein's structural segmentation into distal subdomains, which behave analogously to Einstein oscillators despite their spatial separation. The inherent disorder, characterized by inhomogeneously coupled harmonic oscillators, paradoxically gives rise to spectral order through sharp frequency resonances. These resonances facilitate long-range, coherent coupling between spatially distant protein regions. Energy exchange between subdomains occurs via these coherent resonances, a process enabled by regions of small gradient in the confinement potential, typically in the mid-frequency spectrum. This mechanism leads to a redistribution of vibrational modes, depopulating both high and low-frequency ranges of the phonon branches. Consequently, the observed thermal behavior, particularly at low temperatures, aligns more closely with Einstein model predictions than with the Debye model. In the protein's folded state, this effect manifests as a 'condensation' of the density of states into a broadened, singular peak, representing the resonant modes driven by the confinement potential. This spectral feature suggests an efficient energy transport mechanism across the protein structure, potentially elucidating how proteins rapidly dissipate or transfer energy despite their complex, disordered structure. Understanding this phenomenon could have profound implications for protein function and the design of novel materials with unique thermal and vibrational properties.

E. A Perspective on the Boson Peak

Our findings provide a fresh theoretical perspective on the origin of the Boson Peak - moving beyond viewing it simply as an excess of low-energy vibrational modes. We propose that the Boson Peak emerges from the spectral focusing imposed by the thermal lens effect, more specifically, the rugosity or fluctuation of the confinement potential W promoting small gradient around the mid-band. This fluctuation tends to produce more localized states sharing the same frequency leading to distal resonances promoting coherent transport, and decreasing the number of states at the zone center and edge (Lifshitz tail).

This interpretation aligns with recent studies[18,52] attributing anomalous heat capacity to quasi-localized vibrations in folded atomic chains where the Boson Peak's origin is traced to quasi-localized 1D vibrations resonantly coupled with transverse phonons in glassy materials. Our results also show fair agreement with several seminal works[15–17,53] discussing densities of states, and thermal conductivities typically at temperatures ranging between 10K and 30K[29].

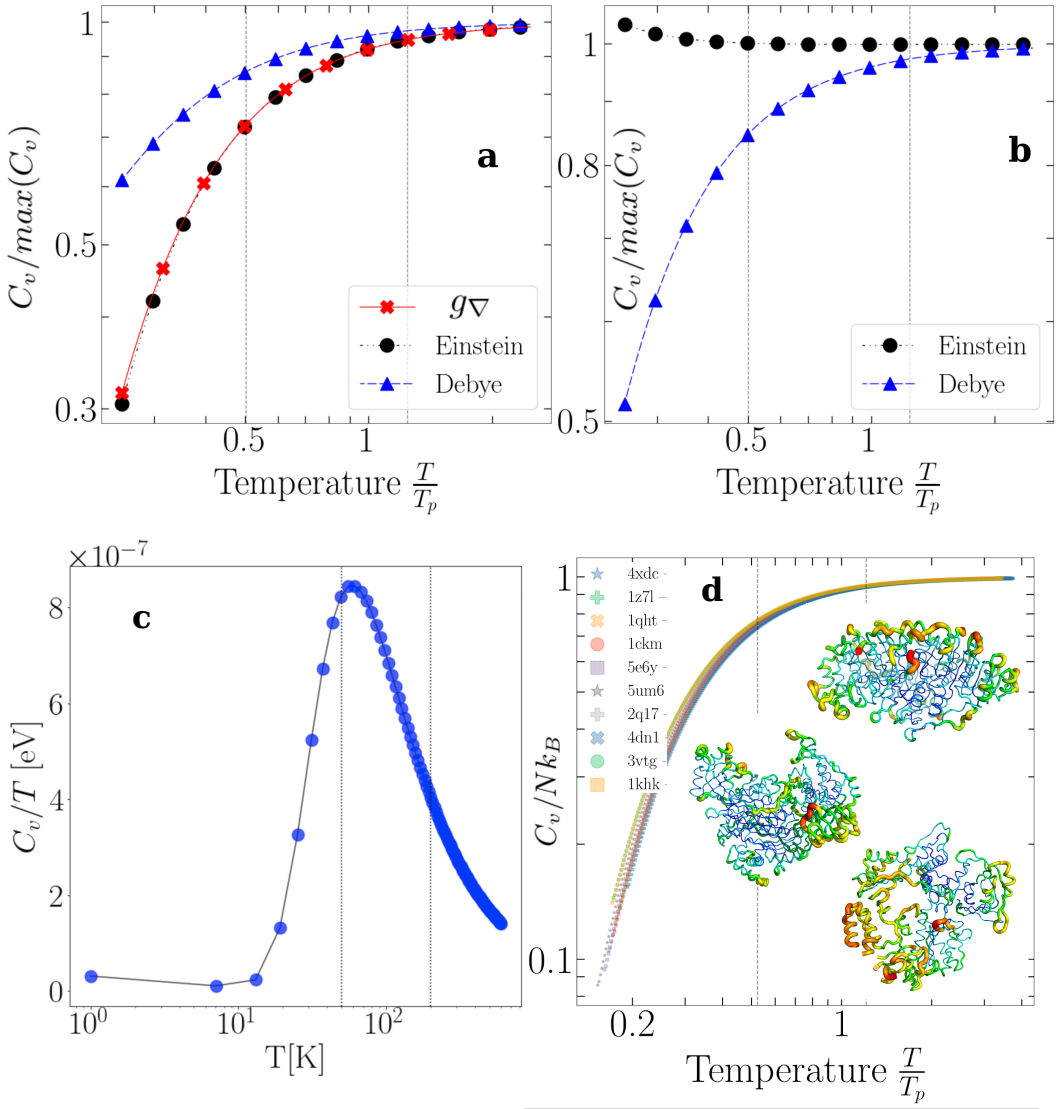

FIG. (4) **Heat Capacity in a disordered phonon structure** a) Compares the heat capacity with the Einstein and Debye approximations, suggesting that the system operates akin to independent Einstein oscillators. Tp corresponds to the thawing temperature of the dominand DOS peak : 135K (for 4xdc). b) Estimates the ratio between the eigenvalues based calculation and the Debye, Einstein models. c) Displays the heat capacity normalized by T, revealing the Boson Peak. Dash lines demarkate the equivalent temperature range of the DOS. d) Demonstrates the universality of the results by estimating $C_v(T)$ for 10 folded proteins, highlighting minimal dispersion although the 3D topologies differ tremendeously (inset).

F. Implications for Condensed Matter Physics

We can extend our results to different types of disorders, including mass variations and bond/elastic constant randomness. As long as these disorders disrupt the dynamical matrix, in a manner where each diagonal element tends to produce an inhomogeneous set of coupled harmonic oscillators, our theory holds. The more inhomogeneous the distribution of oscillators is, the more the effective confinement landscape will fluctuate, increasing the number of localized states. Consequently, this confinement potential will limit coherent phonon paths by spatially distributing energy into few localized domains that do not exchange energy, while thermal transport becomes facilitated in a restricted energy channel instead of a wide frequency range (acoustic branch) in regular solids. The thermal lens concept is crucial in explaining the unique thermal behavior in certain disordered systems. The rugosity or fluctuation of this potential tends to promote Lifshitz tails, resulting in a concentrated phonon density of states and altered heat capacity behavior, facilitating resonant interaction among phonons at the mid-band

where coherent energy transport will predominate.

1. Implications for Material Science

Our observations of the thermal lens effect naturally occurring in proteins provide a rational to advance materials design leveraging this phenomenon. While nature thorough evolution, exploits these thermal effects for regulating biology macromolecular processes[54], we unveil parallel opportunities in engineered systems. The computational tools developed here enable rapid prototype screening to identify polymer structures exhibiting desired heat channeling traits. Specifically, the thermal lensing paradigm establishes prospects for designing insulators that suppress propagation in targeted spectral ranges, logic devices processing information through frequency-selective heat flows, and thermal diodes or transistors gating thermal currents. These diverse applications highlight the breadth of possibilities unlocked by acquiring the ability to deliberately construct and control artificial thermal lenses at the materials scale. Much as nature sculpted thermal landscapes over eons of evolution to regulate biological functions[36,37,54], our framework brings this manifestation of structural disorder into the realm of intentional design.

V. CONCLUSION

This study presents a comprehensive framework for analyzing coherent thermal energy transport in disordered systems, with particular emphasis on folded polymers. By developing analytical tools and theoretical constructs, we have addressed the complex interplay between structural disorder and phonon propagation in non-crystalline materials. This allows us to elucidate the subtle effects of disorder—arising from both topological irregularities and compositional variations—on phonon localization and dissipation mechanisms, and attempts to bridge the gap between theoretical predictions and experimental observations. More specifically, the methodology developed herein establishes correlations between structural characteristics, spectral properties, and thermal transport phenomena in a simplified model of amorphous solids. We believe that this approach also provides a foundation for tailoring thermal conduction in more complex systems. While primarily focused on phonon dynamics, the physical principles underlying this study may have broader implications for understanding energy transport in various amorphous systems. We hope the methodologies and insights presented here open new avenues for investigation in materials science, potentially impacting fields ranging from energy management to materials engineering.

* yann.chalopin@cnrs.fr

[1] R. Peierls, "Zur kinetischen theorie der wärmeleitung in kristallen," Annalen der Physik **395**, 1055–1101 (1929), https://onlinelibrary.wiley.com/doi/pdf/10.1002/andp.19293950803.

[2] Keivan Esfarjani, Gang Chen, and Harold T. Stokes, "Heat transport in silicon from first-principles calculations," Phys. Rev. B **84**, 085204 (2011).

[3] Philip B. Allen and Joseph L. Feldman, "Thermal conductivity of glasses: Theory and application to amorphous si," Phys. Rev. Lett. **62**, 645–648 (1989).

[4] B. L. Zink, R. Pietri, and F. Hellman, "Thermal conductivity and specific heat of thin-film amorphous silicon," Physical Review Letters **96**, 055902 (2006).

[5] Matthew C. Wingert, Jianlin Zheng, Soonshin Kwon, and Renkun Chen, "Thermal transport in amorphous materials: A review," Semiconductor Science and Technology **31**, 113003 (2016).

[6] Taishan Zhu and Elif Ertekin, "Phonons, localization, and thermal conductivity of diamond nanothreads and amorphous graphene," Nano Letters **16**, 4763–4772 (2016).

[7] Weili Liu and Alexander A. Balandin, "Thermal conduction in AlxGa1xN alloys and thin films," Journal of Applied Physics **97**, 073710 (2005), https://pubs.aip.org/aip/jap/article-pdf/doi/10.1063/1.1868876/10658414/073710_1_online.pdf.

[8] Xiaoxi Ni, Meng Lee Leek, Jian-Sheng Wang, Yuan Ping Feng, and Baowen Li, "Anomalous thermal transport in disordered harmonic chains and carbon nanotubes," Phys. Rev. B **83**, 045408 (2011).

[9] Shiqian Hu, Zhongwei Zhang, Pengfei Jiang, Jie Chen, Sebastian Volz, Masahiro Nomura, and Baowen Li, "Randomness-induced phonon localization in graphene heat conduction," The Journal of Physical Chemistry Letters **9**, 3959–3968 (2018), pMID: 29968477, https://doi.org/10.1021/acs.jpclett.8b01653.

[10] Philip B. Allen, Joseph L. Feldman, Jaroslav Fabian, and Frederick Wooten, "Diffusons, locons and propagons: Character of atomie yibrations in amorphous si," Philosophical Magazine B **79**, 1715–1731 (1999).

[11] Wei Lv and Asegun Henry, "Non-negligible contributions to thermal conductivity from localized modes in amorphous silicon dioxide," Scientific Reports **6**, 35720 (2016).

[12] V Vitelli, S Sachdev, and M J Stone, "Spatially localized vibrational modes in amorphous solids," Physical Review Letters **92**, 96301 (2004).

[13] Xi Chen, Annie Weathers, Jesús Carrete, Saikat Mukhopadhyay, Olivier Delaire, Derek A. Stewart, Natalio Mingo, Steven N. Girard, Jie Ma, Douglas L. Abernathy, Jiaqiang Yan, Raman Sheshka, Daniel P. Sellan, Fei Meng, Song Jin, Jianshi Zhou, and Li Shi, "Twisting phonons in complex crystals with quasi-one-dimensional substructures," Nature Communications **6**, 6723 (2015).

[14] M. N. Luckyanova, J. Mendoza, H. Lu, B. Song, S. Huang, J. Zhou, M. Li, Y. Dong, H. Zhou, J. E. Garay, *et al.*, "Phonon localization in heat conduction," Science Advances **4**, eaat9460 (2018).

[15] Mariana F. Ando, Omar Benzine, Zhiwen Pan, Jean-Luc Garden, Katrin Wondraczek, Stephan Grimm, Kay Schuster, and Lothar Wondraczek, "Boson peak, heterogeneity

and intermediate-range order in binary sio2-al2o3 glasses," Scientific Reports **8**, 5394 (2018).

[16] Roman Holomb, Vladimír Tkáč, Vladimir Mitsa, Alexander Feher, and Miklos Veres, "Structural nature of boson peak and low-temperature heat excess in as2s3 glass," physica status solidi (b) **257**, 1900525 (2020), https://onlinelibrary.wiley.com/doi/pdf/10.1002/pssb.201900525.

[17] B. Huang, H. Y. Bai, and W. H. Wang, "Relationship between boson heat capacity peaks and evolution of heterogeneous structure in metallic glasses," Journal of Applied Physics **115**, 153505.

[18] Yuan-Chao Hu and Hajime Tanaka, "Origin of the boson peak in amorphous solids," Nature Physics **18**, 669–677 (2022).

[19] V.K. Malinovsky and A.P. Sokolov, "The nature of boson peak in raman scattering in glasses," Solid State Communications **57**, 757–761 (1986).

[20] V. L. Gurevich, D. A. Parshin, and H. R. Schober, "Anharmonicity, vibrational instability, and the boson peak in glasses," Phys. Rev. B **67**, 094203 (2003).

[21] W. Schirmacher, G. Ruocco, and T. Scopigno, "Acoustic attenuation in glasses and its relation with the boson peak," Phys. Rev. Lett. **98**, 025501 (2007).

[22] Shanshan Chen, Qingzhi Wu, Columbia Mishra, Junyong Kang, Hengji Zhang, Kyeongjae Cho, Weiwei Cai, Alexander A. Balandin, and Rodney S. Ruoff, "Thermal conductivity of isotopically modified graphene," Nature Materials **11**, 203–207 (2012).

[23] A. Marruzzo, W. Schirmacher, A. Fratalocchi, and F. Leonforte, "Boson-peak vibrational modes in glasses feature hybridized phononic and quasilocalized excitations," Physical Review E **90**, 062307 (2014).

[24] Alessia Marruzzo, Walter Schirmacher, Andrea Fratalocchi, and Giancarlo Ruocco, "Heterogeneous shear elasticity of glasses: The origin of the boson peak," Scientific Reports **3**, 1407 (2013).

[25] W. Schirmacher, A. Marruzzo, A. Fratalocchi, and F. Leonforte, "Heterogeneous elasticity: The tale of the boson peak," Physical Review E **102**, 033007 (2020).

[26] Matteo Baggioli and Alessio Zaccone, "Universal origin of boson peak vibrational anomalies in ordered crystals and in amorphous materials," Phys. Rev. Lett. **122**, 145501 (2019).

[27] Kenichiro Mouri and Hajime Tanaka, "Phonon localization and the boson peak in disordered solids," Nature Materials **8**, 149–154 (2009).

[28] T. S. Grigera, V. Martín-Mayor, G. Parisi, and P. Verrocchio, "Phonon interpretation of the 'boson peak' in supercooled liquids," Nature **422**, 289–292 (2003).

[29] R. C. Zeller and R. O. Pohl, "Thermal conductivity and specific heat of noncrystalline solids," Phys. Rev. B **4**, 2029–2041 (1971).

[30] A. J. Minnich, "Thermal transport in disordered materials and its implications on phonon localization," Science Advances **4**, eaat9460 (2018).

[31] Ronggui Xie, Ning Yang, and Gang Chen, "Evidence of phonon anderson localization on the thermal properties of disordered atomic systems," Journal of Applied Physics **130**, 190901 (2021).

[32] Michele Simoncelli, Nicola Marzari, and Francesco Mauri, "Wigner formulation of thermal transport in solids," Phys. Rev. X **12**, 041011 (2022).

[33] W. Zhang, N. Mingo, and T. S. Fisher, "Simulation of phonon transport across a non-polar nanowire junction using an atomistic green's function method," Phys. Rev. B **76**, 195429 (2007).

[34] Leyla Isaeva, Giuseppe Barbalinardo, Davide Donadio, and Stefano Baroni, "Modeling heat transport in crystals and glasses from a unified lattice-dynamical approach," Nature Communications **10**, 3853 (2019).

[35] Marcel Filoche and Svitlana Mayboroda, "Universal mechanism for anderson and weak localization," Proceedings of the National Academy of Sciences **109**, 14761–14766 (2012), https://www.pnas.org/doi/pdf/10.1073/pnas.1120432109.

[36] Y. Chalopin, F. Piazza, S. Mayboroda, and M. Filoche, "Universality of fold-encoded localized vibrations in enzymes," Scientific Reports **9**, 12835 (2019).

[37] Yann Chalopin and Julien Sparfel, "Energy bilocalization effect and the emergence of molecular functions in proteins," Frontiers in Molecular Biosciences **8** (2021), 10.3389/fmolb.2021.736376.

[38] Michele Simoncelli, Francesco Mauri, and Nicola Marzari, "Thermal conductivity of glasses: first-principles theory and applications," npj Computational Materials **9**, 106 (2023).

[39] Lei Yang, Guang Song, and Robert L. Jernigan, "Protein elastic network models and the ranges of cooperativity," Proceedings of the National Academy of Sciences **106**, 12347–12352 (2009), https://www.pnas.org/doi/pdf/10.1073/pnas.0902159106.

[40] See Supplemental Material at URL-will-be-inserted-by-publisher for details in equations derivations.

[41] Hiroshi Matsuda and Kunio Ishii, Progress of Theoretical Physics Supplement **45**, 56–86 (1970).

[42] Douglas N. Arnold, Guy David, David Jerison, Svitlana Mayboroda, and Marcel Filoche, "Effective confining potential of quantum states in disordered media," Phys. Rev. Lett. **116**, 056602 (2016).

[43] Lei Yang, Guang Song, and Robert L. Jernigan, "Protein elastic network models and the ranges of cooperativity," Proceedings of the National Academy of Sciences **106**, 12347–12352 (2009), https://www.pnas.org/doi/pdf/10.1073/pnas.0902159106.

[44] Monique M. Tirion, "Large amplitude elastic motions in proteins from a single-parameter, atomic analysis," Phys. Rev. Lett. **77**, 1905–1908 (1996).

[45] Y. Chalopin, S. P. Cramer, and S. Arragain, "Phonon-assisted electron-proton transfer in [fefe] hydrogenases: Topological role of clusters," Biophys J **122**, 1557–1567 (2023), epub 2023 Mar 23.

[46] J. Esselborn, N. Muraki, K. Klein, V. Engelbrecht, N. Metzler-Nolte, U.-P. Apfel, E. Hofmann, G. Kurisu, and T. Happe, "A structural view of synthetic cofactor integration into [fefe]-hydrogenases," Chem. Sci. **7**, 959–968 (2016).

[47] A. I. Chumakov, G. Monaco, A. Monaco, W. A. Crichton, A. Bosak, R. Rüffer, A. Meyer, F. Kargl, L. Comez, D. Fioretto, H. Giefers, S. Roitsch, G. Wortmann, M. H. Manghnani, A. Hushur, Q. Williams, J. Balogh, K. Parliski, P. Jochym, and P. Piekarz, "Equivalence of the boson peak in glasses to the transverse acoustic van hove singularity in crystals," Phys. Rev. Lett. **106**, 225501 (2011).

[48] I. M. Lifshitz, "Energy spectrum structure and quantum states of disordered condensed systems," Sov. Phys. Usp. **7**, 549–573 (1965).

[49] W. Kirsch and B. Metzger, "Density of states and lifshitz tails for discrete 1d random dirac operators," J. Math. Phys. **48**, 093505 (2007).
[50] L. Erdős and A. Knowles, "Fluctuation corrections to lifshitz tails for the density of states of random schrödinger operators," J. Stat. Phys. **151**, 1003–1022 (2013).
[51] A. H. Chahrour, "Internal lifshitz tails for the density of surface states of random schrödinger operators," J. Math. Phys. **54**, 083303 (2013).
[52] Yuan-Chao Hu and Hajime Tanaka, "Universality of stringlet excitations as the origin of the boson peak of glasses with isotropic interactions," Phys. Rev. Res. **5**, 023055 (2023).
[53] Yu Matsuda, Hitoshi Kawaji, Tooru Atake, Yasuhisa Yamamura, Shuma Yasuzuka, Kazuya Saito, and Seiji Kojima, "Non-debye excess heat capacity and boson peak of binary lithium borate glasses," Journal of Non-Crystalline Solids **357**, 534–537 (2011), 6th International Discussion Meeting on Relaxation in Complex Systems.
[54] Humanath Poudel and David M. Leitner, "Locating dynamic contributions to allostery via determining rates of vibrational energy transfer," The Journal of Chemical Physics **158**, 015101 (2023), https://pubs.aip.org/aip/jcp/article-pdf/doi/10.1063/5.0132089/16661638/015101_1_online.pdf.

ACKNOWLEDGEMENTS

YC is supported by a public grant overseen by the French National Research Agency (ANR) as part of the "Investissements d'Avenir" program (Labex NanoSaclay, reference: ANR-10-LABX-0035). ZT and YC would like to thank the FACE fundation for their financial support.